Spatial resolution enhancement of Earth observation products using an acceleration technique for iterative methods

Flavia Lenti, *Student Member, IEEE,* Ferdinando Nunziata, *Senior Member, IEEE,* Claudio Estatico and Maurizio Migliaccio, *Senior Member, IEEE*

Abstract

A simple innovation that enables faster convergence rate of iterative gradient-like descent approaches is proposed and applied to linear image reconstruction problems from irregular sampling. The key idea is to reduce the amount of regularization effects of the conventional Tikhonov functional by introducing a negative semi-norm penalty term, whose role is to speed-up the convergence without reducing the reconstruction accuracy.
The method is employed to enhance the spatial resolution of microwave remotely sensed products. First experiments, undertaken on simulated radiometer data, demonstrate that the technique significantly increases the convergence rate, halving the number of iterations when applied to speed up the basic and widely used Landweber method.

Index Terms

Spatial resolution enhancement, iterative regularization methods.

I. Introduction

Satellite remote sensing is a key tool for Earth Observation (EO) purposes, resulting in a global view of the Earth. Clouds, forests, land, ocean, ice, etc. can be observed in a very effective way from space. Remote sensing provides typically indirect measurements, i.e. the unknown function is not directly evaluated, but needs to be estimated from few remotely sensed measurements.

F. Lenti is with the Dipartimento di Scienze e Alte Tecnologie, Università degli Studi dell'Insubria, Como, Italy e-mail: flavia.lenti@uninsubria.it

F. Nunziata and M. Migliaccio are with the Dipartimento di Ingegneria, Università degli Studi di Napoli Parthenope, Napoli, Italy e-mail: {ferdinando.nunziata, maurizio.migliaccio} @uniparthenope.it

C. Estatico is with the Dipartimento di Matematica, Università degli Studi di Genova, Genova, Italy e-mail: estatico@dima.unige.it

For a wide class of remote sensing problems, the relationship between the t-th measurement, b_t, and the unknown function, $f(\cdot)$, is described by the Fredholm integral equation of the first kind with a smooth kernel $G_t(\cdot)$:

$$b_t = \int_{\Omega} G_t(y) f(y) dy. \tag{1}$$

Eq. (1) is a linear ill-posed problem. When the kernel is band-limited, (1) can be expressed as [1]:

$$\mathbf{A}_t^T \mathbf{x} = b_t, \tag{2}$$

where $\mathbf{A}_t \in \mathbf{R}^n$ is the conventional sampling of the band-limited kernel G_t and $\mathbf{x} \in \mathbf{R}^n$ is the sampled version of the continuous-index signal $f(\cdot)$. To estimate a band-limited version of $f(\cdot)$ from m measurements $\mathbf{b} = (b_1, ..., b_m)$, the following linear system has to be solved:

$$A\mathbf{x} = \mathbf{b}, \tag{3}$$

where $A = (\mathbf{A}_1, \mathbf{A}_2, ..., \mathbf{A}_m)^T$. The problem may be fully determined, over-determined or under-determined. For most remote sensing applications, A is under-determined. This is the case of spatial resolution enhancement methods that aim at reconstructing the unknown function at a finer resolution. These methods are usually applied to radiometer and scatterometer products, which are characterized by a dense spatial/temporal coverage but poor spatial resolution [1]-[11]. This poor spatial resolution is an applicative limit to the use of these data in coastal zone and enclosed sea or to monitor medium size islands. The resolution of scatterometer/radiometer products can be improved by solving a specific linear inverse problem, which can be considered as the analogue of the antenna-pattern deconvolution. However, since the problem is under-determined, there is no unique solution and an additional constraint must be applied to reconstruct the right unknown function. In addition, due to the ill-posedness of the continuous problem (1), the corresponding eq.(3) is an ill-conditioned discrete problem that requires regularization methods [5].

In the literature, several regularization methods have been proposed to deal with spatial resolution enhancement of microwave remotely sensed products. These methods can be divided into two main categories: direct and iterative.

Direct methods, e.g. Truncated Singular Value Decomposition [3], [4], [5], Tikhonov method [5], [9] and Backus-Gilbert [10], are based on standard decompositions in numerical linear algebra.

Iterative methods, e.g. Landweber method [11], [12], [13], Conjugate Gradient [5], Algebraic Reconstruction Technique (ART) [5], [14] and Scatterometer Image Reconstruction algorithm (SIR) [1], [2], [15], rely on an iterative scheme that converges to the desired solution. Many iterative schemes can be considered as regularization methods, where the iteration number plays the role of regularization parameter. Generally, iterative methods minimize the 2-norm of the residual $A\mathbf{x} - \mathbf{b}$ subject to the minimization of the 2-norm of the energy [5], by means of particular Tikhonov functionals [14]. Iterative methods outperform direct ones when the matrix A is large scale since the former can take advantage of "sparsity" and structure of the matrix more than the latter. However, the key drawback of iterative methods is often a slow convergence rate, as in the case of Landweber method and its generalizations [5], [6].

In this paper, the spectral properties of the integral kernel G are first used to reduce the "amount" of regularization effects of the classical Tikhonov functional. This analysis allows us to define a new functional, whose action is called "de-regularization", which yields acceleration in the first iterations. We first test this new functional by means of the simple Landweber method. Experiments undertaken on simulated radiometer data demonstrate that the de-regularization technique halves the number of iterations without losing reconstruction accuracy and without increasing the numerical complexity of any single iteration. Although we deal with the Landweber method, which is simple and fast to explain and to be implemented, we remark that the idea can be applied to speed up any gradient-like iterative method [7], [8], [11].

Moreover, the proposed method is also contrasted with the popular fixed-point iterative procedure ART [14]. ART is a very computer-time effective algorithm that minimizes the same functional minimized by the classical Landweber method, and it is widely used to enhance the spatial resolution of radiometer data [2]. Experimental results show that the the proposed acceleration technique allows the simple Landweber method to achieve the same performance of ART.

II. Theoretical background

The basic approach to solve (3) consists of minimizing the square of the 2-norm of the residual $A\mathbf{x} - \mathbf{b}$; i.e. minimizing the least square functional Ω_2 defined as [16]:

$$\Omega_2(\mathbf{x}) = \frac{1}{2} \parallel A\mathbf{x} - \mathbf{b} \parallel_2^2 = \frac{1}{2} \sum_{i=1}^{m} (A\mathbf{x} - \mathbf{b})_i^2. \tag{4}$$

Since Ω_2 is a convex differentiable functional and $\nabla\Omega_2(\mathbf{x}) = A^*(A\mathbf{x} - \mathbf{b})$, where A^* denotes the adjoint matrix of A, the solutions of the least squares equation $A^*A\mathbf{x} = A^*\mathbf{b}$ are all global minimum points. However, due to the ill-posedness of (1), a direct solution of the least squares equation leads to high noise amplification; hence, regularization techniques are mandatory. On the other hand, many iterative methods can be often successfully applied to the least squares equation, due to their own regularization capabilities. This regularization effect comes as a result of using a smooth initialization field and restricting the number of iterations, which tends to result in a reconstructed signal with attenuated low signal-to-noise ratio (SNR) components [16].

The simplest class of iterative methods to minimize (4) is the gradient-like one, whose $k-$ th iteration is given by:

$$\mathbf{x}_k = \mathbf{x}_{k-1} - \lambda_{k-1}\mathbf{p}_{k-1} \tag{5}$$

where $\mathbf{x}_0$ is an arbitrary initial guess, $\lambda_{k-1} > 0$ is the so-called step-size, and $\mathbf{p}_{k-1}$ is an ascent direction at point $\mathbf{x}_{k-1}$ for Ω_2; i.e. $\mathbf{p}_{k-1}$ is a vector such that $\langle \nabla\Omega_2(\mathbf{x}_{k-1}), \mathbf{p}_{k-1} \rangle > 0$, with $\langle \cdot, \cdot \rangle$ being the inner product. A wide set of popular iterative methods for the solution of $\nabla\Omega_2(\mathbf{x}) = 0$ belongs to this class, e.g., for $\mathbf{p}_{k-1} = \nabla\Omega_2(\mathbf{x}_{k-1})$ we have the Landweber method (where the step size $\lambda_{k-1} = \lambda \in (0, 2/\|A\|_2^2)$ is constant) and the steepest descent (where any λ_{k-1} is explicitly computed); for $\mathbf{p}_{k-1}$ as special linear combination of $\nabla\Omega_2(\mathbf{x}_{k-1})$ and $\mathbf{p}_{k-2}$, we

have the conjugate gradient. In the same class we can also find special algorithms such as Simultaneous Iterative Reconstruction Techniques (SIRT) [17] and the scaled gradient projection method when a vectorial step size is used [18].

The key drawback of iterative methods is often a slow convergence [5], which limits their operational usage. To speed up the convergence, several sophisticated techniques have been proposed, e.g. preconditioning or Banach spaces model setting. Here, we simply propose to modify the least square functional by subtracting a penalty term that effectively amplifies the components more sensitive to noise effects, allowing a faster and controlled recovering of the noise subspace (i.e., the eigenspace of A^*A related to the vanishing eigenvalues, which corresponds to high frequencies in our inverse problem). This term can be de-weighted as a function of the iteration number, so that the noise amplification of the subsequent iterations is avoided.

To develop the new approach, it is worth recalling a standard case of regularization, where, however, a functional different from (4) is considered:

$$\bar{\Omega}_2(\mathbf{x}) = \frac{1}{2} \parallel A\mathbf{x} - \mathbf{b} \parallel_2^2 + \frac{\alpha}{2} \parallel \mathbf{x} \parallel_S^2, \tag{6}$$

where α is a pre-assigned positive regularization parameter, $\|\mathbf{x}\|_S^2 = \langle S\mathbf{x}, \mathbf{x}\rangle$, and S is a positive semidefinite self-adjoint operator that, in general, may depend on the spectral properties of the operator A. The functional (6) is similar to the classical Tikhonov functional (where $S = I$) and its generalizations. In [19], several operators S have been discussed, and the simplest one we use here is given by

$$S = \left(I - \frac{A^*A}{\parallel A \parallel_2^2} \right), \tag{7}$$

where I is the identity matrix. The definition of S represents a crucial point regarding the impact of (6), because now, differing from all the classical cases where the penalty term is fixed and independent of the operator A, the penalty term depends on A, i.e. it depends on the model problem. We used the 2-norm in (7) since it allows a straightforward interpretation of the role of the operator S as a high-pass filter that vanishes the low frequency components related to the largest eigenvalues of A^*A. Nevertheless, a modified S which uses a more general norm may be used in applications where significant efficiency could obtained by computing a specialized and more easily computable norm, rather than the basic 2-norm (i.e., the largest singular value, whose computation is well known to be often heavy).

To analyze the behaviour of the operator S, the singular value decomposition of $A = U\Sigma V^*$ is used:

$$S = V \left(I - \frac{\Sigma^2}{\sigma_1^2} \right) V^* = V \text{diag}(F(\sigma_1), F(\sigma_2), \ldots, F(\sigma_m)) V^*, \tag{8}$$

where Σ is the diagonal matrix whose elements $\{\sigma_i\}_{i=1,\ldots,m}$ are the descendent-ordered singular values, V is the matrix whose columns are the corresponding right singular vectors and $F(\sigma) = 1 - (\sigma/\sigma_1)^2$. We recall that in the inverse problem (1), the singular value decomposition allows discriminating between signal and noise subspaces. Indeed, smaller σ_i are related to the noise subspace (i.e., the corresponding right singular vectors generate the noise

subspace), while, when σ_i is approaching to σ_1, the right singular vectors generate the signal subspace [5], see Fig.1(a). Hence, $F(\sigma_i)$ vanishes the signal subspace while leaving almost unchanged the noise subspace, so that it really behaves as a A-dependent high-pass filter, see Fig.1(b). This implies that the term $\| \mathbf{x} \|_S^2$ in (6) is large when $\mathbf{x}$ belongs to the noise subspace.

Following this rationale, in literature $\alpha > 0$ is always used to improve the regularization capabilities, since the minimum of the functional (6) gets strong regularity (due to the high values of the penalty term for solutions in the noise subspace). This rationale has been previously exploited to enhance the regularization effectiveness of the classical Tikhonov functional when solved via direct methods, which usually require high stability and high noise filtering [19].

In this study, where only iterative regularization methods are used, a completely different paradigm is proposed, which consists of using $\| \mathbf{x} \|_S^2$ as a "de-regularizing" term. Note that this is the opposite of Tikhonov regularization. Indeed, since we rely on the regularization effect of the iterative procedure itself (which is guaranteed by a smooth initialization and a limited number of iterations), we do not enforce regularization by any penalty term, since it would lead to a de-boosting of the convergence speed. This means that, when using iterative regularization methods, the additional penalty term of (6) can be often neglected since further regularization is not useful. On the contrary, if the iterative method is too slow, in general it has too high regularization effectiveness, which should be reduced in order to speed-up the convergence. Accordingly, a parameter $\alpha < 0$ is used in (6), in order to reduce the regularization in the first iterations, so that therein the convergence speed is improved. Specifically, this negative parameter is what we term as "de-regularization". We explicitly point out that, to the best of our knowledge, this is the first time that a negative penalty term is adopted. This leads to a new functional $\bar{\Omega}_2$ that, being a difference of convex functionals, is a delta-convex functional [20].

Due to the explicit form of $\nabla\bar{\Omega}_2(\mathbf{x}) = A^*(A\mathbf{x}_{k-1} - \mathbf{b}) + \alpha S\mathbf{x}_{k-1}$, we now analyze the technique in the simplest case of Landweber method. Starting from $\mathbf{x}_0 = \mathbf{0}$, the Landweber iterative scheme applied to (6) becomes:

$$\mathbf{x}_k = \mathbf{x}_{k-1} - \lambda A^*(A\mathbf{x}_{k-1} - \mathbf{b}) - \beta_k S\mathbf{x}_{k-1} \tag{9}$$

where $\lambda = (0, 2/\|A\|_2^2)$ and $\beta_k = \lambda\alpha_k \leq 0$. In the following, we call the algorithm (9) as *improved Landweber method*. Here the parameter (α_k) specifies the weight α of the penalty term in $\nabla\bar{\Omega}_2$ at iteration k. The selection of the zero-th iteration $\mathbf{x}_0 = \mathbf{0}$ guarantees that any other $\mathbf{x}_k$ belongs to the subspace orthogonal to the null-space of A. Note that the same applies when the weaker hypothesis $\mathbf{x}_0 \in \text{Null}(A^*A)$ is satisfied. The larger is $|\beta_k|$, the stronger is the weight of the penalty term subtracted in (6) at iteration k. Note that to make the final result less affected by noise amplification resulting from a large de-regularization, the parameter $\beta_k \leq 0$ is a function of the iteration number and goes to zero asymptotically. A first convergence result is the following [21]:

Theorem Let (α_k) be a sequence of real numbers $\alpha_k \leq 0$ such that $\sum_k \alpha_k$ converges. If $\lambda \in (0, 2/\sigma_1^2)$, then the sequence $(\mathbf{x}_k)$ given by the improved Landweber method (9) with $\mathbf{x}_0 \in \text{Null}(A^*A)$ and de-regularization parameters

$\beta_k = \alpha_k \lambda \leq 0$, converges to the Moore-Penrose generalized solution $\mathbf{x}^\dagger$ of the linear equation (3); i.e. the minimum norm solution.

By a simple manipulation of (9):

$$\mathbf{x}_k = (1 - \beta_k)\mathbf{x}_{k-1} - A^*((\lambda - \beta_k \parallel A \parallel_2^{-2})A\mathbf{x}_{k-1} - \lambda \mathbf{b}). \tag{10}$$

It can be noted that the computational cost of each iteration of the improved Landweber method is the same of the conventional one.

Even if we apply the "de-regularization" rationale to the simple Landweber method, we remark that any gradient-like iterative method can be straightforwardly accelerated according to the above-mentioned theoretical rationale. Moreover, in a more general view, the iteration-dependent de-regularizing term can be even incorporated directly into the cost function of any iterative method that is specialized to the radiometer/scatterometer problem (e.g., the Fieldwise Estimation or SIR algorithm [1]), leading to specific accelerated versions of recent real algorithms of high impact. Furthermore, the output of the improved Landweber can be also used as starting guess of more sophisticated algorithms.

III. Numerical Results

In this section, numerical experiments are discussed to evaluate the proposed acceleration technique based on the minimization of the modified functional (6) with de-regularizing parameters $\alpha = \alpha_k \leq 0$. Hence, the improved Landweber method (10) that represents the simplest example of application of the acceleration technique, is employed to enhance the spatial resolution of simulated Special Sensor Microwave/Imager (SSM/I) radiometer measurements. Improved Landweber is compared with conventional Landweber method and with ART [14], which is used in [2] to enhance the spatial resolution of radiometer data. Note that the latter two methods minimize the same standard functional (4). According to [5], ART parameters are chosen to obtain the best trade-off between the noise filtering and convergence rate.

The SSM/I is a conical scan microwave seven-channel radiometer whose swath is about 1400 km. It performs 64 measurements along with the along-scan direction and 28 scans with a 25 km pixel spacing [22]. The t-th measurement is given by (1) where $f(\cdot)$ is the unknown brightness temperature and $G_t(\cdot)$ is the projection of the integrated antenna pattern on the surface that can be approximated by a two-dimensional Gaussian function [4].

In the first test, a 1400×700 km reference field is simulated, then the noisy measurements are obtained using (3) and a zero-mean Gaussian additive noise, whose standard deviation is equal to 1.06 K, corresponding to a noise level of about 10%[15]. This noise model is the standard one used to address spatial resolution enhancement of radiometer data, see e.g. [1]-[4], [9]-[11], [15]. In this study, the iterative methods are applied to reconstruct the brightness field of Fig. 2(a) from the SSM/I measurements shown in Fig. 2(b). The rationale related to the simulation

of the SSM/I brightness field and the spatial resolution enhancement using conventional Landweber method is fully detailed in [11].

The discrepancy principle [5] is used to stop the iterations in an objective and unsupervised way. It consists of choosing the smallest iteration number k such that:

$$\| A\mathbf{x}_k - \mathbf{b} \|_2 \leq c, \tag{11}$$

where c is an estimate of the 2-norm of the noise. To evaluate the reconstruction accuracy, we adopt the relative error defined as [4]:

$$err_k = \frac{\| \mathbf{x}_k - \mathbf{x}_{ref} \|_2}{\| \mathbf{x}_{ref} \|_2}, \tag{12}$$

where $\mathbf{x}_k$ is the vectorized version of the k -th iteration reconstructed field and $\mathbf{x}_{ref}$ is vectorized version of the reference true field.

According to the Theorem of the previous section, to guarantee the convergence, a k-dependent choice β_k has be to used. In this paper, the following rule is adopted:

$$\beta_k = -\frac{\beta_0}{2^{k-1}} \tag{13}$$

with $\beta_0 \geq 0$. For $\beta_0 > 0$, $|\beta_k|$ is a decreasing function of k that results in a "de-regularizing" term (see eq. (6)) that tends towards 0 for increasing k, while for $\beta_0 = 0$, the conventional Landweber method is obtained. Moreover, since $\beta_k = \lambda\alpha_k$ with the relaxation parameter $\lambda = 1/\sigma_1^2$, the sequence $\sum_k \alpha_k = -\beta_0\lambda^{-1}\sum_k 2^{1-k}$ converges, so the hypotheses of the convergence theorem of previous section are fulfilled.

The residuals obtained using the decreasing sequences (13) with $\beta_0 = 0, 2^1, 2^3, 2^5$ are plotted in Fig. 3(a) where they are contrasted with the residual obtained by the ART. The residuals for both $\beta_0 = 0, 2^1, 2^3$ and ART are monotonic decreasing functions with k, saturating (11) at $k = 121, 120, 68$ and 65 respectively. Hence, one can note that for increasing β_0 the number of iterations to saturate (11) reduces and for $\beta_0 = 2^3$ the iteration number is very similar to the ART one. Differently, when $\beta_0 = 2^5$ the residual is no longer monotonic, showing a convex behaviour. This occurrence can be experienced for any other β_0 values larger than 2^5. This is due to the fact that too much regularity is subtracted within first iterations. Indeed, this can be theoretically explained by noting that the functional (6) consists of two terms: the residual and the "de-regularizing" term. Although the functional $\bar{\Omega}_2$ is minimized, the contribution of the "de-regularizing" addendum may outperform the residual one, so that the residual can diverge even if the functional converges.

The relative errors (12) are plotted versus k in Fig. 3(b). It can be noted that, for a fixed k, $\beta_0 > 0$ results in relative errors generally smaller than $\beta_0 = 0$. This demonstrates that the improved Landweber method, i.e. $\beta_0 > 0$, outperforms the conventional Landweber method. For $\beta_0 = 2^3$ the relative error is very similar to the ART one. It can be noted that using $\beta_0 = 2^3$, after 10 iterations the third term at the right-hand side of eq.(9) becomes negligible. Hence, one may think that the conventional Landweber regularization scheme is achieved. This is actually untrue,

since a completely different $\mathbf{x}_{k-1}$ term is obtained. In fact, after 10 iterations, the relative error is equal to 0.71 and 0.95 for the improved and the conventional Landweber methods respectively.

To further investigate the reconstruction accurancy of the conventional Landweber ($\beta_0 = 0$) and the improved one ($\beta_0 = 2^3$), the two methods are applied to reconstruct the brightness field of Fig.2(a) and the iteration is stopped when the residual is no longer monotonic descendent. The reconstructed field that corresponds to the minimum error is shown in Fig.5(a) and (b) for $\beta_0 = 0$ and $\beta_0 = 2^3$, respectively. The relative error is 0.53 in both the cases and it is reached at $k = 175, 120$ for $\beta_0 = 0$ and $\beta_0 = 2^3$, respectively. In addition, it can be noted that no artifacts are introduced by the improved Landweber.

The results are confirmed by several experiments, not shown to save space. To further discuss the effectiveness of the proposed approach against scenarios that include abrupt and smooth discontinuities, two experiments are undertaken using the reference fields shown in Fig.5. For each reference field, two Gaussian noises whose standard deviations are 1.06 and 0.6, respectively, are considered and the fields are then reconstructed from noisy measurements using both the conventional ($\beta_0 = 0$) and the improved ($\beta_0 = 2^3$) methods. The objective norm and the number of iterations to saturate (11) are listed in Table I. The obtained results confirm that the improved Landweber method outperforms the conventional one in terms of computation time, without affecting the reconstruction accuracy.

IV. Conclusion

A new paradigm to allow faster convergence rate is proposed for iterative regularization gradient-like descent approaches. The key idea consists of modifying the conventional least square functional by subtracting a penalty term. This subtraction acts as a de-regularization, yielding acceleration in the first iterations. This negative penalty term is then de-weighted as a function of the iteration number to avoid noise amplification in the subsequent iterations. The accelerated version of the Landweber method is compared with the conventional one and with the popular ART method. Experiments demonstrate the effectiveness of the accelerated Landweber method which results in a number of iterations: a) halved with respect to the conventional Landweber method; b) similar to the one obtained using the ART. The proposed acceleration technique can be applied to other widely used gradient-like regularization iterative methods. A natural development line after this first proposal could be also to include both a regularizing term and a de-regularizing term in the functional to minimize. The latter term should dominate the first few iterations only, and should become negligible as the iterations increase, thus ensuring regularization and allowing a noise/resolution trade-off, while shaping the error trajectory to fall off faster for the beginning iterations.

Acknowledgement

The authors would like to thank the anonymous reviewers for their useful suggestions. The work of C. Estatico is partly supported by MIUR, PRIN 2012 n. 2012MTE38N.

REFERENCES

[1] B.A. Williams and D.G. Long, "Reconstruction from aperture-filtered samples with application to scatterometer image reconstruction," *IEEE Trans. Geosci. Remote Sens.*, vol. 49, no. 5, pp. 1663-1675, 2011.

[2] D.S. Early and D.G. Long, "Image reconstruction and enhanced resolution imaging from irregular samples," *IEEE Trans. Geosci. Remote Sens.*, vol. 39, no. 2, pp. 291-302, 2001.

[3] M. Migliaccio and A. Gambardella, "Microwave radiometer spatial resolution enhancement," *IEEE Trans. Geosci. Remote Sens.*, vol. 4, no. 5, pp. 1159-1169, 2005.

[4] F. Lenti, F. Nunziata, M. Migliaccio, and G. Rodriguez, "Two-dimensional TSVD to enhance the spatial resolution of radiometer data," *IEEE Trans. Geosci. Remote Sens.*, vol. 52, no. 5, pp. 2450-2458, 2014.

[5] P.C. Hansen, *Rank-deficient and discrete ill-posed problem: numerical aspects of linear inversion*. Philadelphia: SIAM, 1987, ch. 6-7, pp. 132-208.

[6] I. Daubechies, M. Defrise, C. De Mol,"An iterative thresholding algorithm for linear inverse problems with a sparsity constraint," *Comm. Pure Appl. Math.*, vol. 57, no. 11, pp. 1413-1457, 2004.

[7] S. Fourcart, H. Rauhut, *A Mathematical Introduction to Compressive Sensing*, NY: Heidelberg: Birkhauser, 2013.

[8] Y.V. Shkvarko, J. Tuxpan, S.R. Santos, "$l2$–$l1$ Structured Descriptive Experiment Design Regularization Based Enhancement of Fractional SAR Imagery," *Signal Proc.*, vol. 93, pp. 3553-3566, 2013.

[9] A. Gambardella and M. Migliaccio, "On the superresolution of microwave scanning radiometer measurements," *IEEE Geosci. Remote Sens. Lett.*, vol. 5, no. 4, pp. 796-800, 2008.

[10] G.E. Backus and J.F. Gilbert, "Numerical applications of a formalism for geophysical inverse problem," *Geophys. J.R. Astr. Soc.*, vol. 13, pp. 247-276, 1967.

[11] F. Lenti, F. Nunziata, C. Estatico, and M. Migliaccio, "On the spatial resolution enhancement of microwave radiometer data in Banach spaces," *IEEE Trans. Geosci. Remote Sens.*, vol. 52, n. 3, pp. 1834-1842, 2014.

[12] C. Bockmann and A. Kirsche, "Iterative regularization method for lidar remote sensing," *Computer Physics Communication*, vol. 174, no. 8, pp. 607-615, 2006.

[13] C. Estatico, M. Pastorino, and A. Randazzo, "A novel microwave approach based on regularization in Lp Banach spaces," *IEEE Trans. Antennas Propag.*, vol. 60, no. 7, pp. 3373-3381, 2012.

[14] H.H. Barrett and K.J. Myers, *Foundations of image science*. New York: Willey, 2004, ch. 1-15.

[15] D.G. Long, "Reconstruction and resolution enhancement techniques for microwave sensors," in *Frontiers of remote sensing information processing*, C.H.Chen, World Scientific, 2003, ch.11.

[16] M. Bertero and P. Boccacci, *Introduction to Inverse Problems in Imaging*. Bristol: Institute of Physics Publ, 1998, ch. 4-5, pp. 73-120.

[17] T. Elfving, T. Nikazad, P. C. Hansen, "Semi-convergence and relaxation parameters for a class of SIRT algorithm". *Elect. Trans. on Num. Anal.*, vol. 37, pp. 321–336, 2010.

[18] S. Bonettini, R. Zanella, L. Zanni, "A scaled gradient projection method for constrained image deblurring". *Inverse Problems.*, vol. 25, no. 1, 2009.

[19] T. Huckle and M. Sedlacek, "Tykhonov-Phillips regularization with operator dependent seminorms," *Numerical Algorithms*, vol. 60, pp. 339-353, 2012.

[20] L. Vesely and L. Zajíček, *Delta-convex mappings between Banach spaces and applications*. Dissertationes Math., vol. 289, 1989.

[21] P. Brianzi, F. Di Benedetto, C. Estatico, L. Surace, "Acceleration of iterative reconstruction methods by de-regularization," *in preparation*, 2014.

[22] J.P. Hollinger, *DMSP Special sensor Microwave/Imager User's Guide*. Washigton D.C.: Naval Res. Lab., 1987.

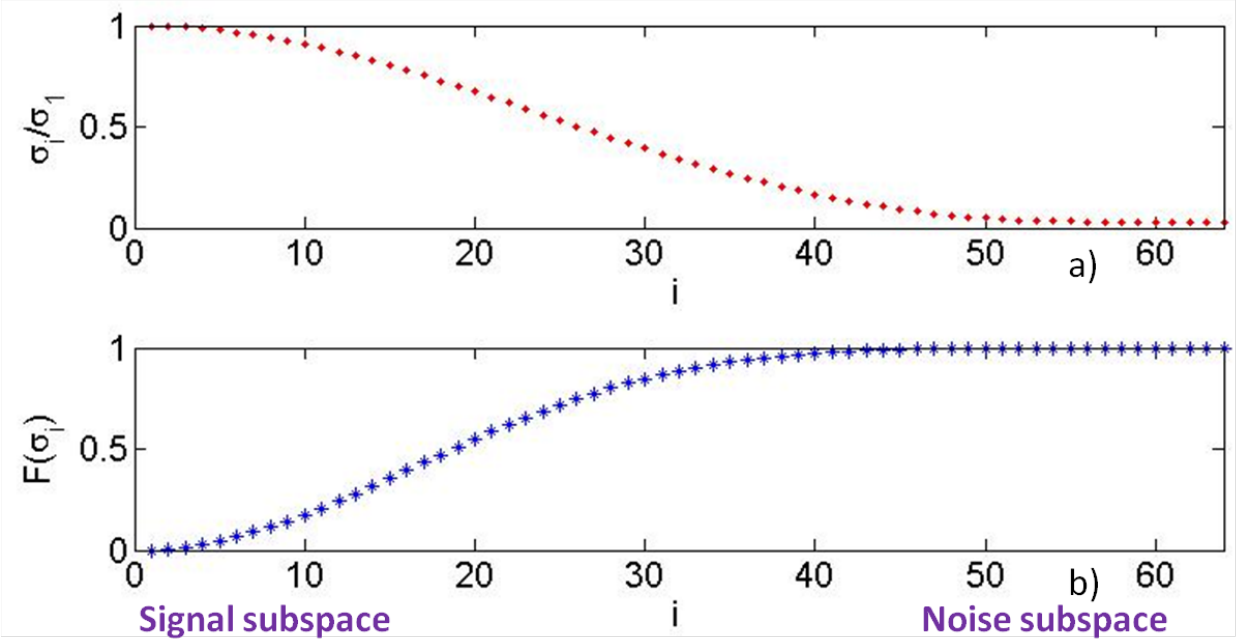

Fig. 1. a) Sketch of normalized singular values of A, that is $\frac{\sigma_i}{\sigma_1}$ for $i = 1, \ldots, rank(A)$. b) Sketch of $F(\sigma_i) = (1 - \frac{\sigma_i}{\sigma_1})$ (8) for varying $i \in [1, ..., rank(A)]$ for $i = 1, \ldots, rank(A)$.

TABLE I

ITERATION NUMBER TO SATURATE THE DISCREPANCY PRINCIPLE (11) AND THE RELATIVE ERROR.

Reference	Noise	$\beta_0 = 2^3$		$\beta_0 = 0$	
Field	std (K)	Iteration Number	Relative Error	Iteration Number	Relative Error
Fig.5(a)	1.06	95	1.2194	175	1.2187
Fig.5(a)	0.6	180	0.8005	220	0.8000
Fig.5(b)	1.06	52	0.8691	93	0.8695
Fig.5(b)	0.6	304	0.7052	515	0.7052

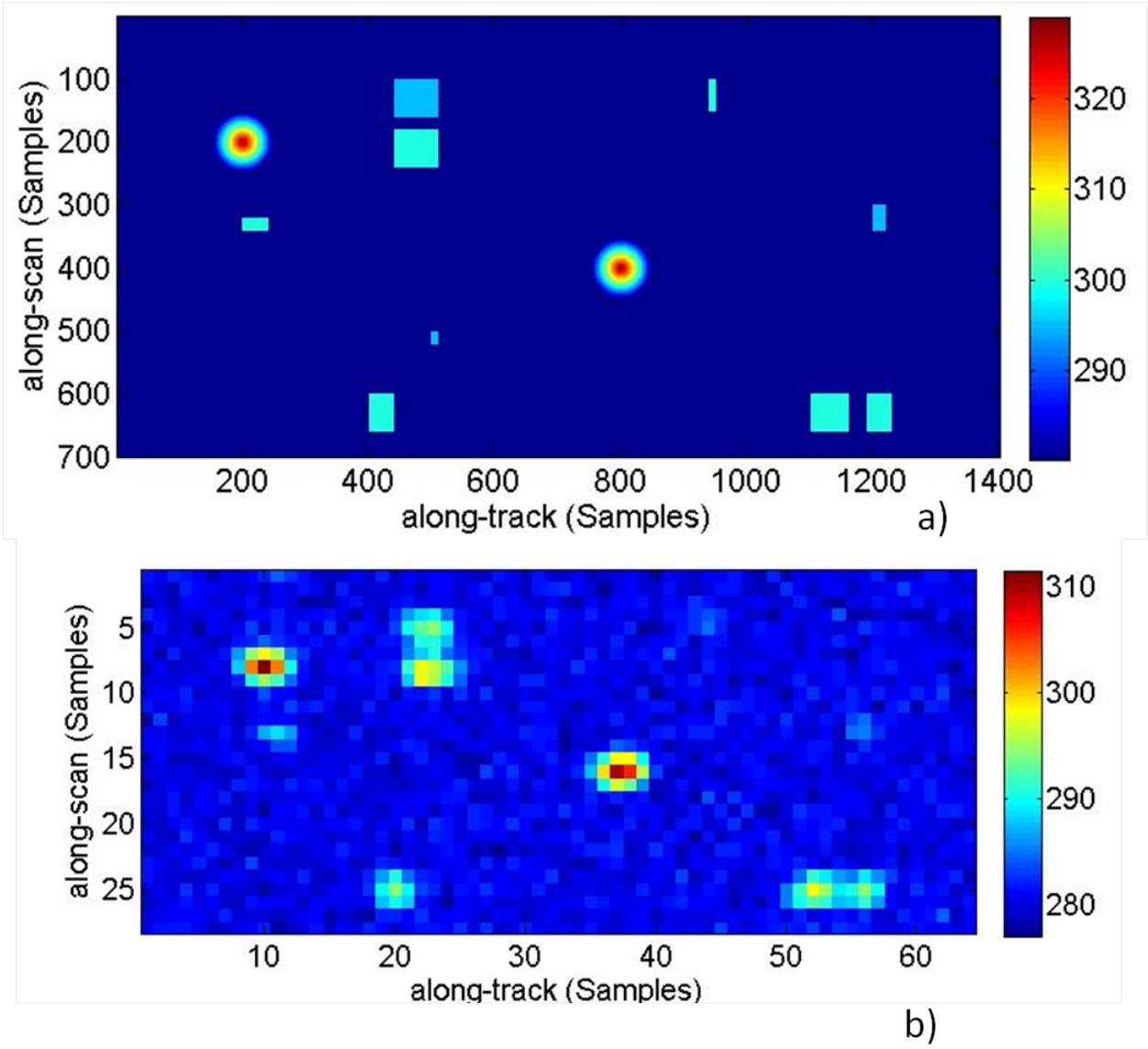

Fig. 2. a) Reference field related to an area of 1400×700 km where some discontinuities of different size and brightness temperature values are presented. b) Simulated noisy measurements obtained by considering SSM/I parameters and 1.06 K additive noise.

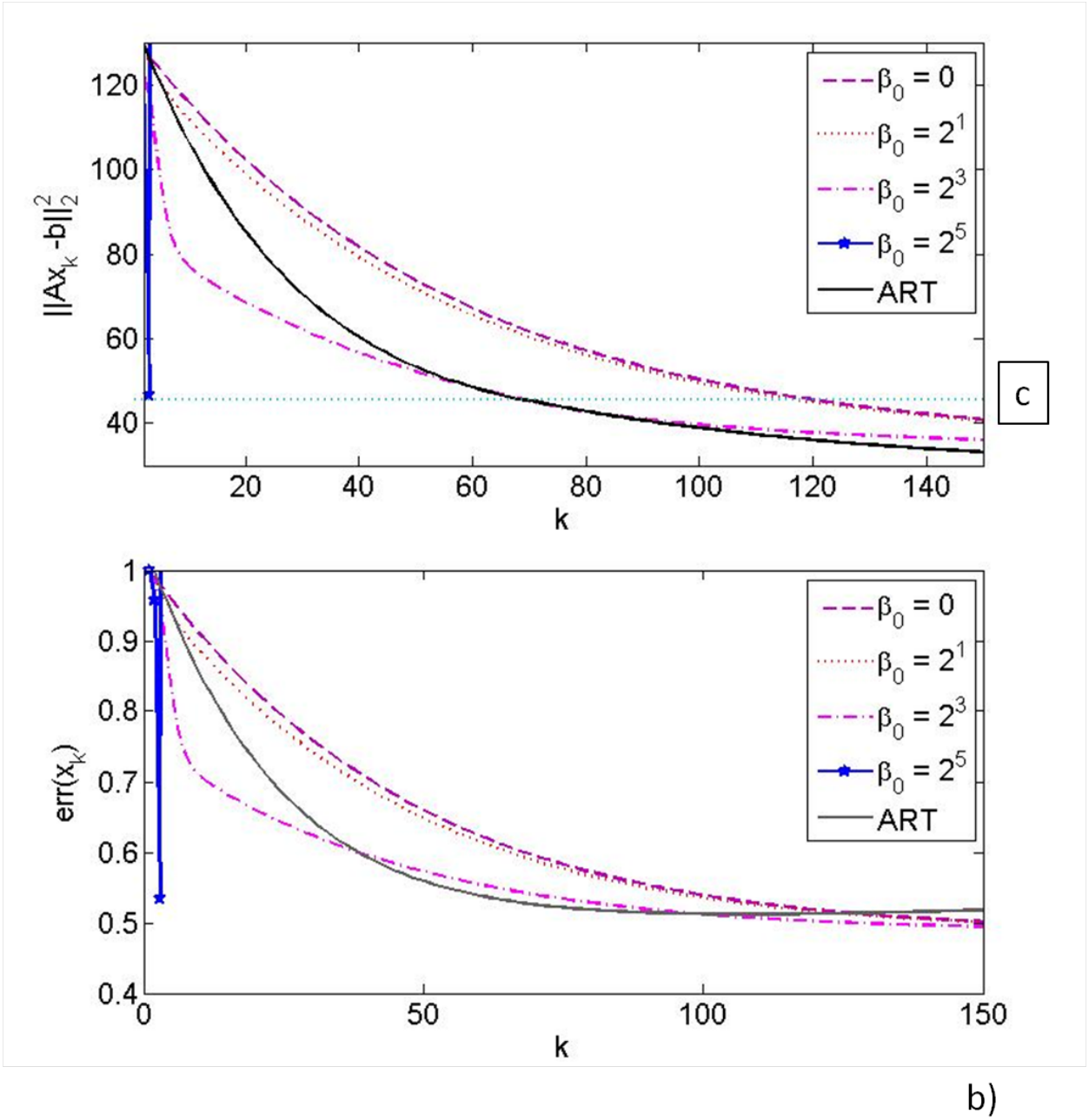

Fig. 3. a) The 2-norm of the residual versus k. b) The relative error between the k-reconstructed and the reference field versus k. c is an upper bound related to the 2-norm of the noise.

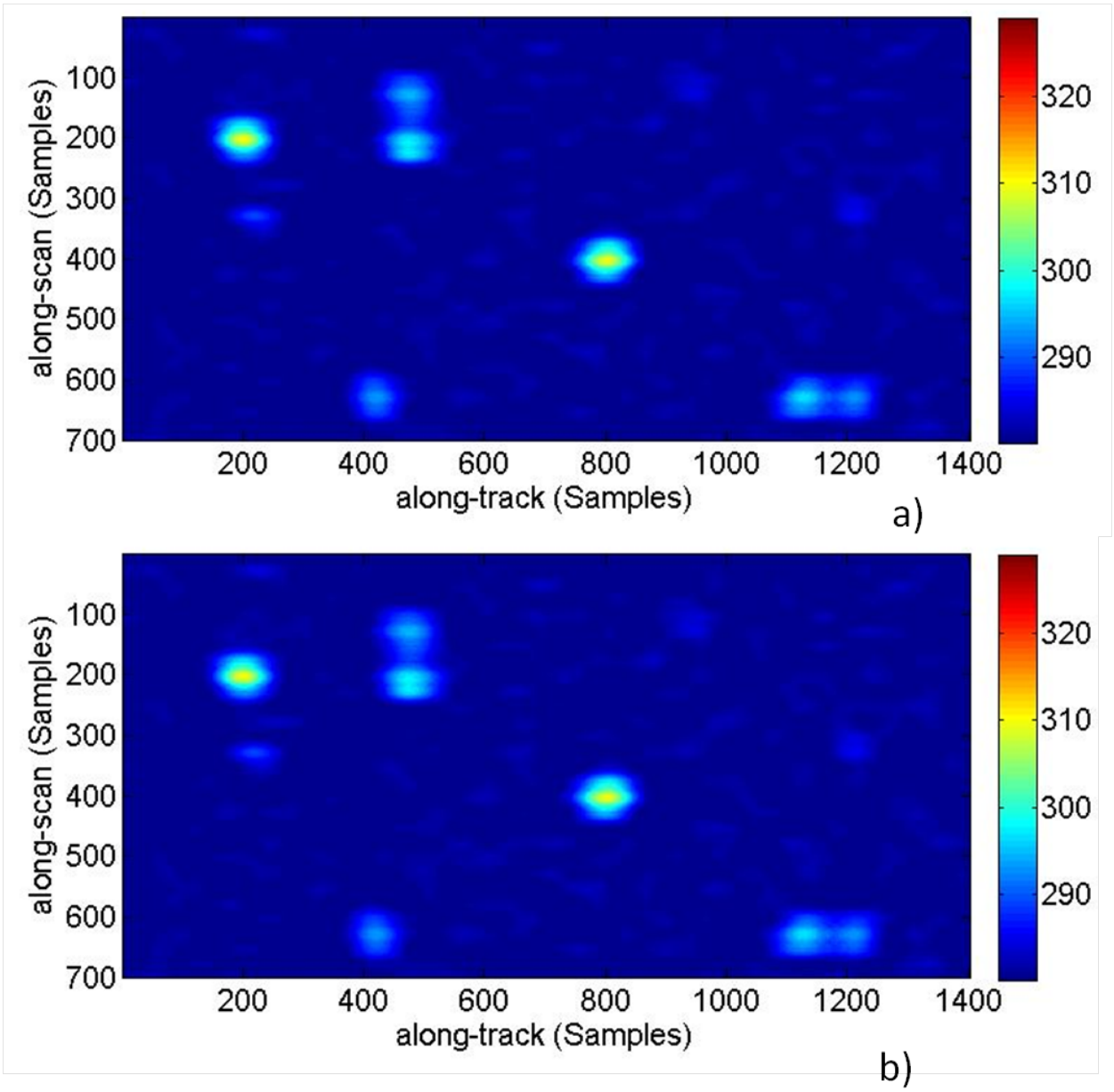

Fig. 4. Reconstructed field using a) the conventional ($\beta_0 = 0$) and b) the improved ($\beta_0 = 2^3$) Landweber method.

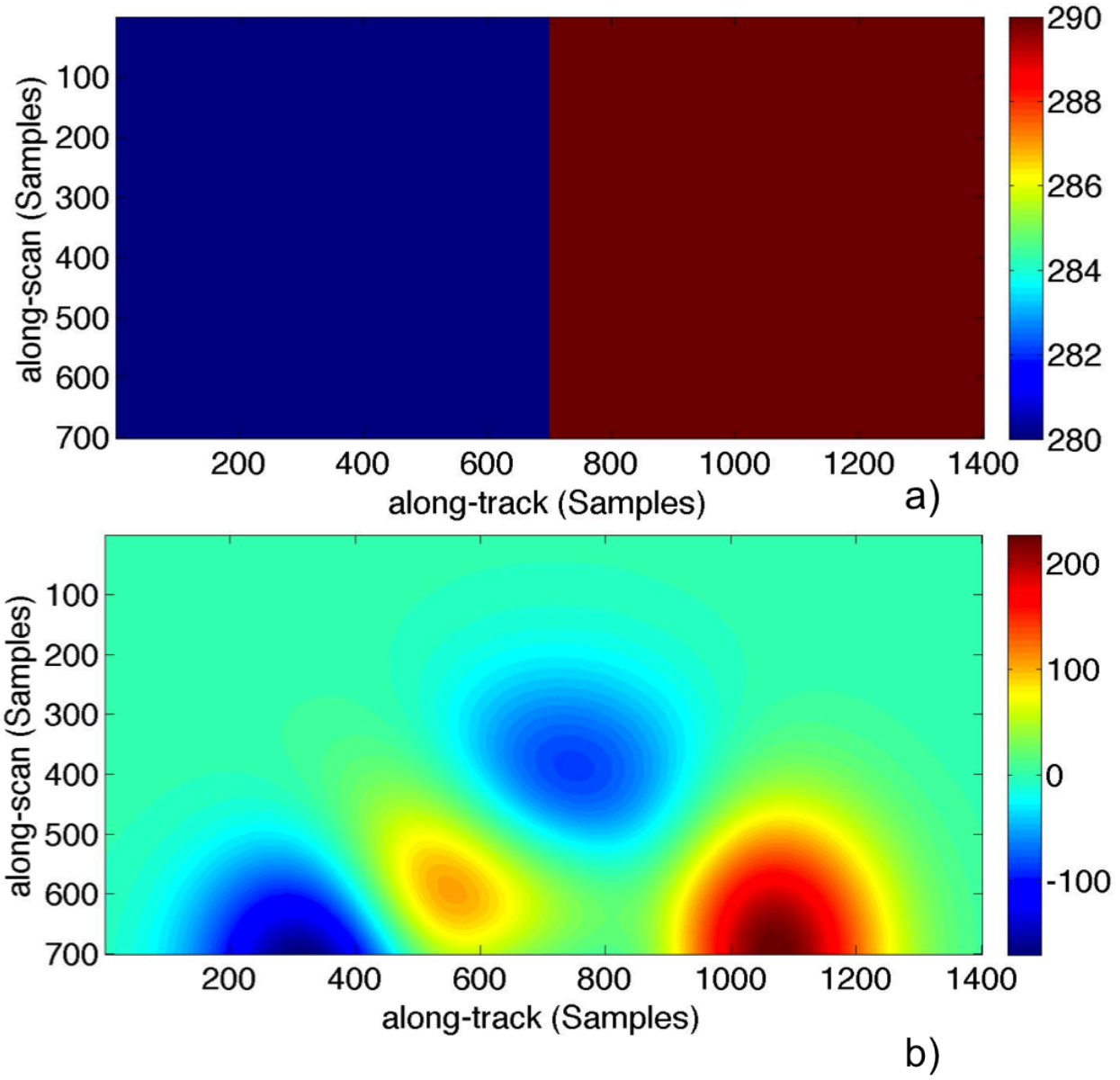

Fig. 5. Reference field related to an area of 1400×700 km where an abrupt discontinuity is presented. b) Reference field related to an area of 1400×700 km where smooth discontinuities are presented.